Comparison of low complexity C/N_0 estimators for GNSS signals affected by ionospheric scintillation

José Marçal[+], Fernando Nunes[+], Fernando Sousa[*]
Instituto de Telecomunicações and IST[+]/ISEL[*]
e-mails: jose.marcal@ieee.org, nunes@lx.it.pt, fsousa@cc.isel.ipl.pt

BIOGRAPHIES

José Marçal received his MSc Degree in Electrical Engineering at Instituto Superior Técnico (IST), University of Lisbon. He is currently pursuing a PhD in Electrical Engineering at the University of Lisbon in the field of vector structures for GNSS receivers. His interests include signal processing in GNSS receivers and sensor fusion. He has worked before as a Project Engineer at NAV Portugal, in projects related to optimization in air traffic control.

Fernando Nunes received the PhD degree in Electrical Engineering from the Instituto Superior Técnico (IST), University of Lisbon, Lisbon, Portugal. He is currently an Assistant Professor at the Department of Electrical and Computer Engineering, IST, and a Researcher with the Communication Theory Group at the Instituto de Telecomunicações, Lisbon. His current research interests include communication theory and signal processing in mobile communications and radio-navigation systems.

Fernando Sousa received the PhD degree in Electrical Engineering from the Instituto Superior Técnico (IST), University of Lisbon, Portugal. He is currently a Coordinator Professor in the Electronics, Telecommunications, and Computer Engineering Department, ISEL, and a Researcher with the Communication Theory Group, Instituto de Telecomunicações, Lisbon. His main research interests include communication theory and signal processing in mobile communications and radio-navigation systems.

ABSTRACT

The C/N_0 estimators in Global Navigation Satellite System (GNSS) receivers were originally proposed for environments where the changes of the GNSS signal power due, for instance, to the varying satellite elevation angle and shadowing effect, are relatively slow. However, the scenarios corresponding to the presence of ionospheric scintillation become much more demanding for the receiver tracking loops as the amplitude and phase of the affected signals experience fast and strong variations. Typically, amplitude deep fades may occur at rates above 1 Hz. The goal of this paper is to analyze the performance of those estimators when the signals are disturbed by scintillation. Several modifications are proposed in the paper in order to maintain the functionality of those algorithms; namely, by replacing the conventional averaging operation with Kalman smoothing.

1 INTRODUCTION

Ionospheric scintillation is a phenomenon produced when the wave propagates through a ionosphere volume with electronic density irregularities, leading to refraction and diffraction of the incident wave, and originating random group delay and phase advance. These contributions generate constructive or destructive effects on the signal, which are sensed by a GNSS receiver as fluctuating signal amplitude and phase, leading to poor ranging performance and possibly provoking carrier loss of lock.

The estimation of the carrier-to-noise ratio (C/N_0) is important in GNSS receivers as it is used to determine whether the receiver is operating normally or is in a region where it is prone to lose carrier lock. In receivers that monitor the activity of the ionosphere in environments affected by scintillation, the instantaneous C/N_0 estimation is crucial to evaluate the scintillation index S_4 [1]. The index is defined as

$$S_4 = \sqrt{\frac{\langle I^2 \rangle}{\langle I \rangle^2} - 1} \tag{1}$$

where $\langle \cdot \rangle$ denotes the time average operator (typically over the period of 60 seconds) and I is the normalized intensity of the scintillation effect such that

$$C/N_0 = \overline{(C/N_0)} I \tag{2}$$

with $\overline{(C/N_0)}$ denoting the average value of the C/N_0 over the averaging period. In the literature, different statistical distributions of the amplitude fading $\sqrt{I}$ are considered, including Nakagami-m, Rice, Rayleigh, and generalized gamma.

Several (C/N_0) estimators have been proposed with emphasis on the narrowband wideband power ratio estimator (NWPR) proposed by Dierendonck in [3]. The papers of Falletti et al. [4] and Islam et al. [6] analyze the performance of various low complexity C/N_0 estimators. All the estimators assume as input the

International Technical Symposium on Navigation and Timing (ITSNT) 2017
14-17 Nov 2017
ENAC, Toulouse, France

responses of the inphase/quadrature prompt correlators. Therein, the evaluation concerns the performance in normal conditions where the C/N_0 is expected to change relatively slowly compared with the scenarios of ionospheric scintillation, where sudden amplitude and phase changes occur very often.

Therefore, it would be interesting to analyze the estimators described in [4] and [6] in environments of ionospheric scintillation, as the ones observed near the geomagnetic equator or in the polar regions. Obviously, the operation of averaging that was used by the estimators in order to diminish the variance of the estimation errors has to be avoided, otherwise the estimates would be too much smoothed to have any practical application. Instead, we propose in this paper to apply a stochastic smoother based on the Kalman filter [5], [8]. The smoothing strategy requires that the samples are processed off-line and was adopted, for instance, in [1]. The advantage of smoothing relative to the Kalman filtering is that the estimation delays are eliminated. The simulation results obtained with the smoothing algorithm show that it is possible to track the instantaneous C/N_0 with good accuracy except, possibly, during very deep fades where the estimators may exhibit significant errors. However, at those low C/N_0 values, even a sophisticated receiver tends to lose carrier lock [2], thus precluding the computation of reliable C/N_0 estimates.

In order to generate simulated signals affected by scintillation, a toolbox provided by T. Humphreys, with the results present in [2] is used. It assumes a Rician distribution for the amplitude and is used as a common source for comparing results with other methods. An important parameter is the correlation time τ that can model the amplitude's rate of change, and is required by the model used. With the values of S_4 and τ, samples can be generated that are a good approximation of typical scintillation scenarios. This is the model used in the simulations presented in this article.

An example of the C/N_0 time sequence generation with Rician distribution for the amplitude is shown in Figure 1, for $\overline{C/N_0} = 40dB - Hz$ with $S_4 = 0.5$ and 0.75.

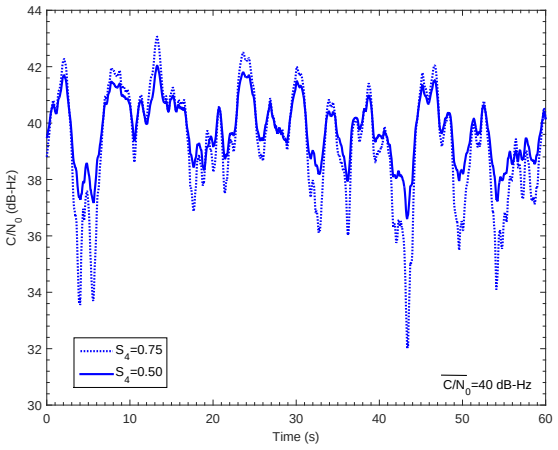

Figure 1: Examples of the C/N_0 time sequence generation with $S_4 = 0.5$ and 0.75.

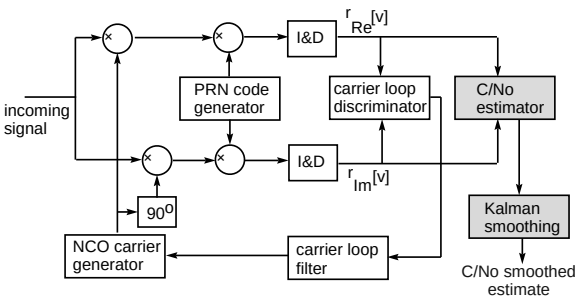

Figure 2: Diagram showing the phase and C/N_0 estimation blocks in the receiver (the DLL is omitted for simplicity).

2 PROBLEM STATEMENT

Figure 2 shows the relevant part of the receiver's structure (only one channel is visible) with the part concerning the delay-lock loop (DLL) being omitted for simplicity. In this work we will focus on the gray blocks, which are the ones related to the C/N_0 estimation. In the next subsections a brief description of the models used is shown.

2.1 Signal description

Consider that the received GNSS signal is

$$r(t) = A(t)c(t)d(t)\cos(\omega_0 t + \omega_d t + \theta) + w(t) \qquad (3)$$

where $A(t)$ is the amplitude of the modulated signal, $c(t)$ is the code signal (possibly associated with a baseband digital modulation), $d(t)$ is the sequence of navigation data, ω_0 and ω_d are, respectively, the carrier and Doppler frequencies, θ is an unknown phase, and $w(t)$ is Gaussian noise with power spectral density $G_w(f) = N_0/2$. Assume a conventional receiver constituted by a bank of DLLs that track the code delay and a bank of PLLs that track the phase of the incoming signals. The complex signal at the output of the inphase/quadrature correlators of the PLL unit, for an integration interval T_{int}, is described as

$$r[n] = \sqrt{P_d}.D[v] + \sqrt{P_n}.\eta[v] \qquad (4)$$

where P_d is the power associated to the received GNSS signal. P_n is the noise power with $\eta = \eta_{Re} + j\eta_{Im}$ being a complex variable that represents the noise present at the inphase and quadrature channels. The r.v. η_{Re} and η_{Im} are independent, zero mean, Gaussian, with common variance N_0/T_{int}.

Assuming perfect code synchronization, $D[v]$ includes the navigation bit samples with a_v dependent on the modulation scheme used and the residual car-

rier phase error θ_v, according to

$$D[v] = a_v.e^{j\theta_v} \tag{5}$$

2.2 C/N_0 estimators

In order to estimate the C/N_0 from the correlator outputs, a selection of low complexity estimators based on [4] and [6] are used. These estimators try to estimate independently the data power and the noise power through different methods. Without loss of generality, we will assume that we are working with GPS C/A signals, and in the algorithms we use a set of N samples $r[v]$ for estimation, with N being the same for all the considered estimators.

2.2.1 Beaulieu's method

In this method the noise power is considered small when compared to the data power. The signal-plus-noise power at the sample v is given by

$$\hat{P}_{d,v} = \frac{1}{2}\left[(r_{Re}[v])^2 + (r_{Re}[v-1])^2\right] \tag{6}$$

and the noise power can be estimated from two consecutive inphase samples:

$$\hat{P}_{n,v} = (|r_{Re}[v]| - |r_{Re}[v-1]|)^2 \tag{7}$$

The value of C/N_0 is then estimated as

$$\frac{C}{N_0} = \frac{1}{T_{int}}\left[\frac{1}{N}\sum_{v=1}^{N}\frac{\hat{P}_{n,v}}{\hat{P}_{d,v}}\right]^{-1} \tag{8}$$

2.2.2 Squared Signal-to-Noise Variance (SSNV) method

In this method we estimate the data power and the total power of the signal from the correlator output. If the phase tracking error is small enough (this assumption becomes worse with lower carrier to noise ratios), the data power can be approximated by

$$\hat{P}_d = \left[\frac{1}{N}\sum_{v=1}^{N}|r_{Re}[v]|\right]^2 \tag{9}$$

while the total power of the signal takes into account the inphase and quadrature components

$$\hat{P}_t = \frac{1}{N}\sum_{v=1}^{N}|r[v]|^2 \tag{10}$$

Therefore, the noise power can be computed from the difference of the total power and the data power

$$\hat{P}_n = \hat{P}_t - \hat{P}_d \tag{11}$$

and the estimate of the C/N_0 is

$$\frac{C}{N_0} = \frac{1}{T_{int}}\frac{\hat{P}_d}{\hat{P}_n} \tag{12}$$

2.2.3 Moments method

A method that shows good results in environments where the data power does not dominate absolutely the noise power is the moments method. It estimates the second and fourth order moments of the r.v. $r[v]$, that is, $M_2 \equiv E\{|r[v]|^2\}$ and $M_4 \equiv E\{|r[v]|^4\}$, by using the following time averages

$$\hat{M}_2 = \frac{1}{N}\sum_{v=1}^{N}|r[v]|^2 \tag{13}$$

$$\hat{M}_4 = \frac{1}{N}\sum_{v=1}^{N}|r[v]|^4 \tag{14}$$

The signal power estimates are thus computed as

$$\hat{P}_d = \sqrt{2\hat{M}_2^2 - \hat{M}_4} \tag{15}$$

and the noise power estimates as

$$\hat{P}_n = \hat{M}_2 - \hat{P}_d \tag{16}$$

The estimate of the carrier to noise ratio from the data and noise power follows the same expression.

2.2.4 Narrowband-Wideband Power Ratio (NWPR) Method

It is a commonly used estimator, proposed in [3], that is used as the reference technique. The narrowband-wideband power ratio method evaluates the total power of the process $r[n]$ in two different bandwidths: a wideband estimate, taken over a noise bandwidth $1/T_{int}$, where T_{int} is the integration time

$$WBP[k] = \sum_{v=1}^{N}|r[kN+v]|^2 \tag{17}$$

and a narrowband estimate, taken over a bandwidth $1/(NT_{int})$, given by

$$NBP[k] = \left(\sum_{v=1}^{N} r_{Re}[kN+v]\right)^2 + \left(\sum_{v=1}^{N} r_{Im}[kN+v]\right)^2 \tag{18}$$

With these two estimates, a random variable is defined as

$$NP[k] = \frac{NBP[k]}{WBP[k]} \tag{19}$$

with expected value

$$\mu_{NP} = E\{NP[k]\} = \frac{\frac{C}{N_o}NT_{int}+1}{\frac{C}{N_o}T_{int}+1} \tag{20}$$

The estimated carrier-to-noise ratio is then given by

$$\frac{C}{N_0} = \frac{1}{T_{int}}\frac{\mu_{NP}-1}{N-\mu_{NP}} \tag{21}$$

To diminish the variance of the C/N_0 estimates using (21) further averaging of the r.v. $NP[k]$ is advisable,

leading to typical values around 1 second for the estimates update interval. However, in scintillation scenarios this strategy cannot be used as we shall discuss later on.

2.2.5 Islam's method (first order)

As in [6] consider

$$z_p = \frac{1}{N}\sum_{v=1}^{N}|r(v)|^2 \tag{22}$$

and

$$z_o = \frac{1}{N}\sum_{v=1}^{N}|\widetilde{r}(v)|^2 \tag{23}$$

where $\widetilde{r}(v) = \widetilde{r}_{Re}(v) + j\widetilde{r}_{Im}(v)$ is the output of an early or late inphase/quadrature correlator with sufficiently large advance or delay regarding the prompt correlator such that only noise is obtained.

The estimated carrier to noise ratio is given by

$$\frac{C}{N_0} = \frac{1}{T_{int}}\frac{z_p - z_o}{z_o} \tag{24}$$

Figure 3 displays the performance of the different C/N_0 estimators under analysis for a constant closed loop phase error $\theta_n = 5^o$. Note that all the estimators except the SSNV produce good estimates above approximately 32 dB-Hz for $T_{int} = 1$ ms and $N = 20$ regardless of the phase error. In contrast, the SSNV estimator is very sensitive to θ_n and saturates for large values of C/N_0. Thus, it has to be excluded from the study as the receivers affected by ionospheric scintillation tend to present significant phase errors, which are not tracked by the PLL. For $C/N_0 < 32$ dB-Hz the estimators exhibit different behaviors with the NWPR showing the best performance. A good estimation in this region is important in scintillation scenarios during deep amplitude fades.

2.3 Kalman Smoothing

The estimation of C/N_0 in receivers where the incoming signals are affected by scintillation cannot be processed, as in nominal conditions, by averaging the estimates over a long time (typically larger than 1 second), due to the fast changes in the amplitude and phase of the incoming signals.

A common approach to this problem is to use Kalman filtering (as in [2]), with the state variable x representing C/N_0 in dBHz. We model its dynamics as a Brownian motion in log domain:

$$x_{n+1} = x_n + w \tag{25}$$

where w is a Gaussian white noise process.

The measurement $y[n]$ is the estimated carrier-to-noise ratio measured in dB using one of the methods described above, with additive white noise $v[n]$. In order to improve the estimates, and for non real-time

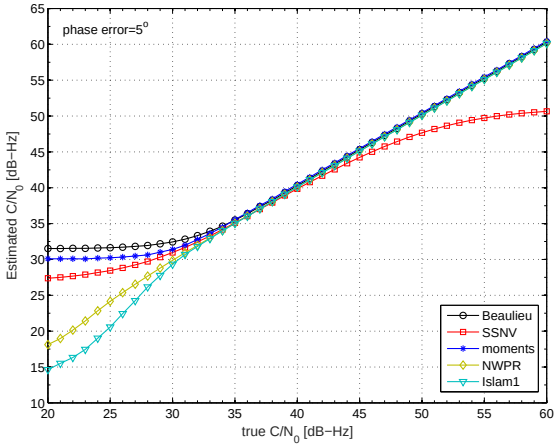

Figure 3: Performance comparison of the analyzed C/N_0 estimators for a constant phase error of 5^o.

applications, the usage of a Kalman smoother leads to better results, as it computes the optimal estimation for each point based on past and future samples, using all the knowledge available.

Three types of smoothing are, in general, considered [8]. Essentially, the equations of two Kalman filters (KF) are propagated in reverse directions: the forward (conventional) KF and the backward KF. In fixed-interval smoothing, the initial and final times 0 and T_f are fixed and the estimate $\hat{x}(t|T_f)$ is determined, with t varying from 0 to T_f. In fixed-point smoothing, t is fixed and $\hat{x}(t|T_f)$ is computed as T_f increases. In fixed-lag smoothing, $\hat{x}(t-\Delta|t)$ is computed as t increases but Δ is held fixed. In this work a fixed-interval Kalman smoother is used, which obtains the optimal estimate from a batch of all the available measurements ($M+1$ observations). The algorithm next described was proposed by Rauch, Tung, and Striebel in [9].

i) The filtering step

$$\hat{x}_{k|k} = \hat{x}_{k|k-1} + K_k(z_k - H_k\hat{x}_{k|k-1}) \tag{26}$$

with the Kalman gain being

$$K_k = P_{k|k-1}H_k^T[H_kP_{k|k-1}H_k^T + R_k]^{-1} \tag{27}$$

where $P_{k|k-1}$ is the covariance matrix of the prediction step, H_k is the observations matrix, and R_k is the measurements noise covariance matrix. In (26), z_k is the observation at iteration k. The update of the filtering step covariance matrix is

$$P_{k|k} = [I - K_kH_k]P(k|k-1), \quad k = 0, \ldots, M \tag{28}$$

The prediction step of the forward KF is given by

$$\hat{x}_{k+1|k} = \Phi_k \hat{x}_{k|k} \tag{29}$$

$$P_{k+1|k} = \Phi_k P_{k|k} \Phi_k^T + Q_k \tag{30}$$

where Q_k is the covariance matrix of the dynamics model noise.

ii) Smoothed state estimate:

$$\hat{x}_{k|M} = \hat{x}_{k|k} + A_k[\hat{x}_{k+1|M} - \hat{x}_{k+1|k}] \tag{31}$$

where

$$A_k = P_{k|k} \Phi_k^T P_{k+1|k}^{-1}, \quad k = 0, \ldots, M-1 \tag{32}$$

and Φ_k is the state transition matrix of the forward KF.

iii) Error covariance matrix propagation:

$$P_{k|M} = P_{k|k} + A_k[P_{k+1|M} - P_{k+1|k}]A_k^T, \quad k = 0, \ldots, M-1 \tag{33}$$

Notice that the measurements z_k appear only in the equations of the forward KF (see equation (26)). For the problem in hand the state and observations vectors are scalar. Besides, $\Phi_k = 1$, $Q_k = q$, $R_k = r$ and the filtering and prediction matrices, respectively $P(k|k)$ and $P(k+1|k)$, are also scalar.

3 SIMULATION RESULTS

In order to test the performance of the proposed algorithm some simulations were performed, assuming a static user. A model of the receiver was used, with the loop filters of the PLLs having a bandwidth of 15 Hz, while the loop filters of the DLLs have a bandwidth of 0.5 Hz. The sampling rate of the discriminators' output is equal to 1000 Hz (integration interval: $T_{int} = 1$ ms) and the rate at which the smoother is updated is 50 Hz (sampling interval: 20 ms). This means that the number of samples used for the accumulation in all the estimators is $N = 20$.

The plots in Fig. 4 compare the estimated (instantaneous) C/N_0 obtained with the Beaulieu, moments, NWPR, and Islam1 estimators with the true values (black line) for $\overline{C/N_0} = 42$ dB-Hz and $S_4 = 0.75$. The results were provided by the Kalman smoother with parameters $q = 100$ and $r = 16$.

Simulations have shown that, within a large range of values of q and r, the Kalman smoother performance depends mainly on the ratio q/r, with smaller values leading to a less "noisy" solution but preventing the smoother from tracking conveniently sudden C/N_0 changes, as it happens with the deep fades.

3.1 C/N_0 estimation for different values of S_4

In Figure 5 the average bias (mean error) of the estimated C/N_0 is plotted versus $\overline{C/N_0}$ for different values

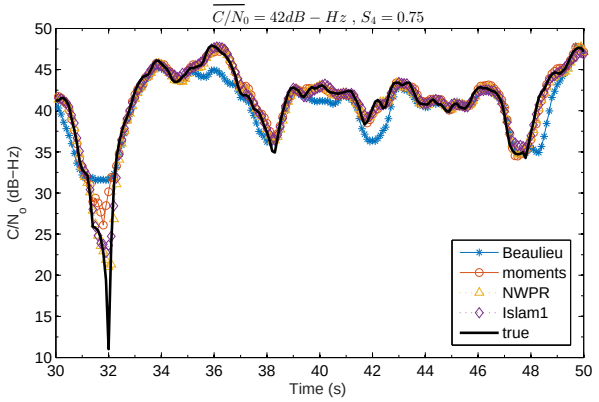

Figure 4: Values of C/N_0 obtained with different estimators for $\overline{C/N_0} = 42$ dB-Hz and $S_4 = 0.75$.

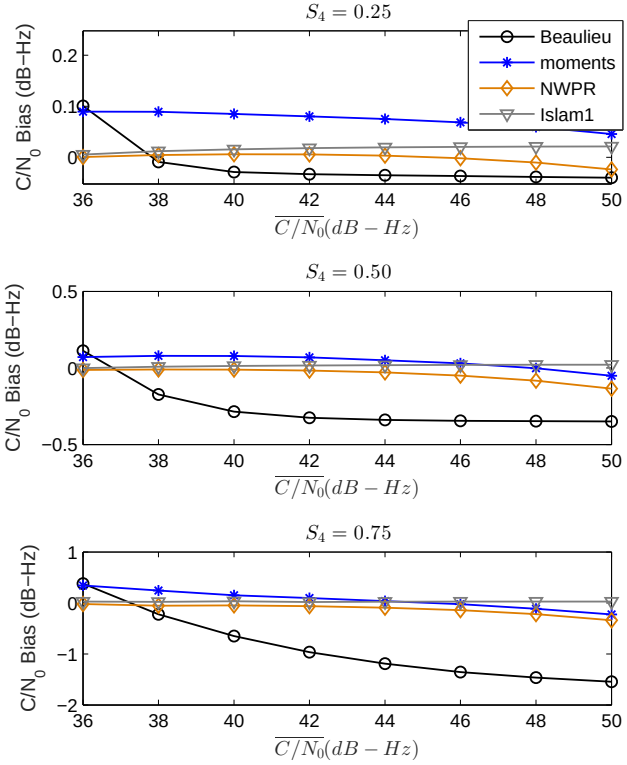

Figure 5: Bias of the C/N_0 estimates versus $\overline{C/N_0}$ for different estimators and S_4 values.

of S_4. It is interesting to notice that the Beaulieu's estimator shows a greater sensitivity to the variation of S_4 in terms of the average error. Islam's first order method seems to be less affected by the different values of S_4, as it does not resort to the inphase and quadrature samples at the correlation peak to estimate the noise power.

In spite of this, a study of the root mean square (rms) errors is important to characterize each method. Figure 6 depicts the rms errors versus $\overline{C/N_0}$ for the same

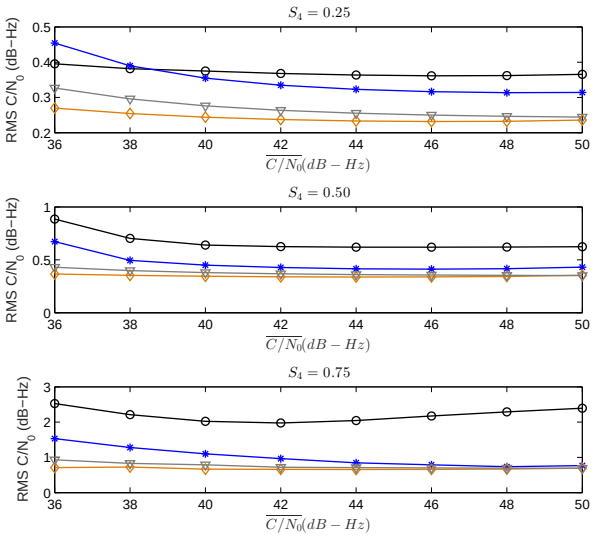

Figure 6: Estimation rms errors of the C/N_0 estimates versus $\overline{C/N_0}$ for different estimators and S_4 values.

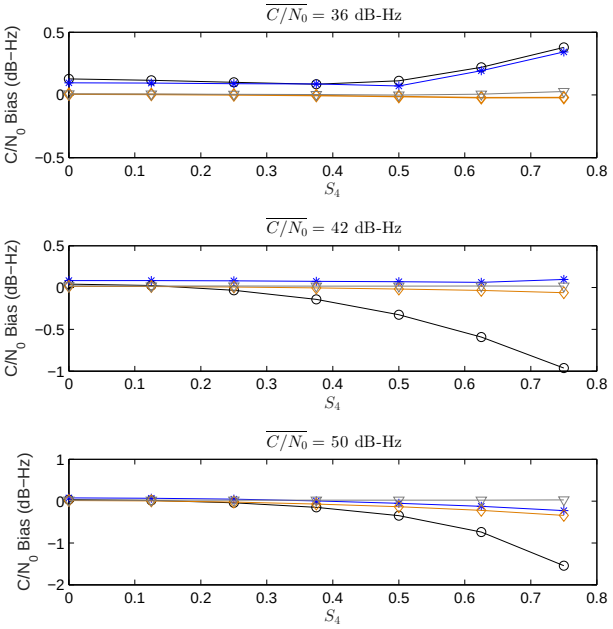

Figure 7: Bias of the C/N_0 estimates versus $\overline{C/N_0}$ for different estimators and S_4 values.

set of S_4 values (assume the same legend as in Fig.5). For other lower $\overline{C/N_0}$ values and low values of S_4, the NWPR method is clearly better, but the first order Islam's method is also comparable. The performance of the moments method when compared to the latter two methods is similar at higher values of S_4, however, for lower values there is a significant difference. The number of samples, limited to $N = 20$ in the scenarios proposed (as the scintillation phenomena does not allow for more relaxation due to the high dynamics) leads to a computation of the moments that may be not as accurate, providing worse C/N_0 estimation results.

A similar problem affects the Beaulieu's estimator, where the accumulation of only 20 samples and posterior inversion does not result in so accurate measurements.

3.2 C/N_0 estimation for different values of average C/N_0

In Figure 7 the average bias of the estimated C/N_0 is plotted versus S_4 for different values of $\overline{C/N_0}$, using the legend shown in Fig. 5. The NWPR and Islam1 estimators are bias free, and the moments estimator shows also good results (only for lower C/N_0 values there is a a slight bias, which is expected as shown in [4]), while the Beaulieu's method tends to be biased as S_4 increases, for all the simulation scenarios.

Figure 8 depicts the rms errors versus S_4 for the same set of $\overline{C/N_0}$ values. It is clear that the first order Islam's method and the NWPR method show consistently better performances (at lower C/N_0 values the NWPR is marginally better), while the moments method improves the performance with respect to C/N_0 rms error as $\overline{C/N_0}$ increases. The Beaulieu's method shows again a more severe degradation in the performance as S_4 increases.

3.3 Kalman smoother performance

Finally, a study of the Kalman smoother performance for different values of $\overline{C/N_0}$ and S_4 was done. In the simulations, we kept the value of the noise covariance r constant, and made the process dynamics equal to $q = 100$ and $q = 1000$.

Figure 9 shows the estimator's performance when the values of S_4 change, for $\overline{C/N_0} = 42$ dB-Hz. In this case, for lower values of S_4 there is a consistently better performance for $q = 100$, but as the value of S_4 goes over 0.6, the process noise increases, and the figure shows that the rms errors tend to be the same for the two smoothers for all the estimators. This suggests a need for an adaptive Kalman filter when the scintillation intensity is high. This is particularly true for the cases of deep fading, when the estimators struggle to keep with the real variation of the C/N_0.

Figure 10 exhibits the results of a simulation set with $S_4 = 0.75$ and varying $\overline{C/N_0}$. For lower values of S_4, a consistently better performance is observed for one type of estimator, but in this case, the increased process dynamics due to the scintillation effect (deep fading, especially) leads to different best estimators, depending on the $\overline{C/N_0}$. Nevertheless, the NWPR estimator shows an overall better performance, with the Islam's method being also a good choice for $\overline{C/N_0}$ values larger than 42 dB-Hz.

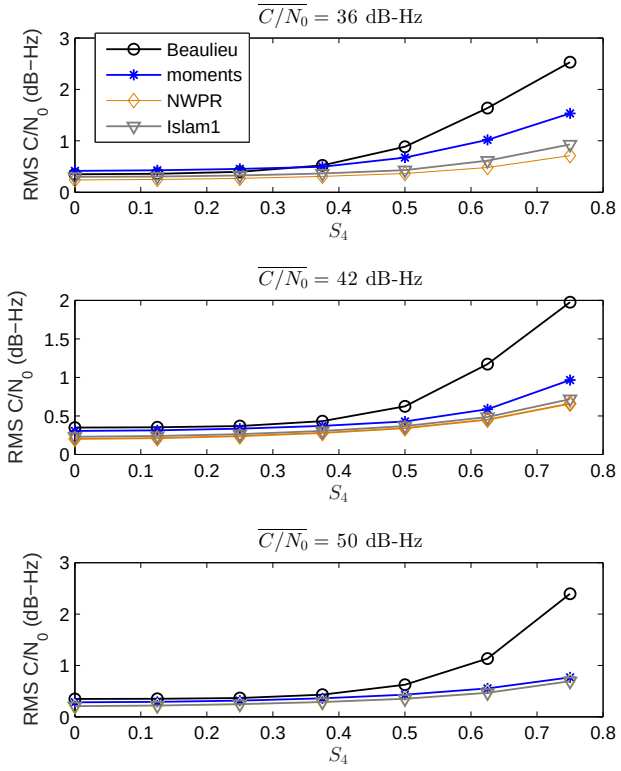

Figure 8: Estimation rms errors of the C/N_0 estimates versus S_4 for different estimators and $\overline{C/N_0}$ values. In the last plot the NWPR and the Islam1 methods are coincident.

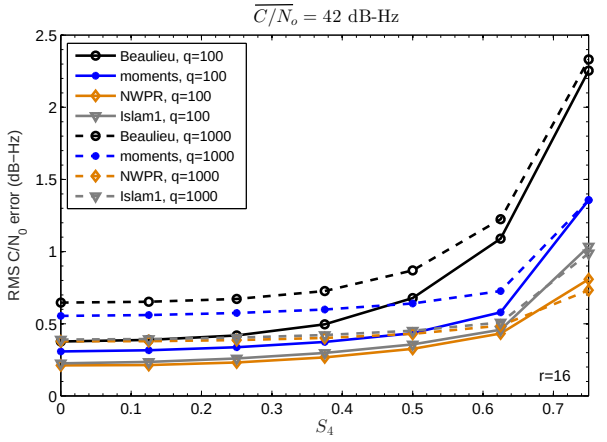

Figure 9: Estimation rms errors of the C/N_0 estimates for different estimators and S_4 values.

4 CONCLUSION

In this article an analysis of the performance of four different types of C/N_0 estimators is performed, when the signals are disturbed by ionospheric scintillation. A Kalman smoother was used with all the methods, allowing to compare the results with simulated values

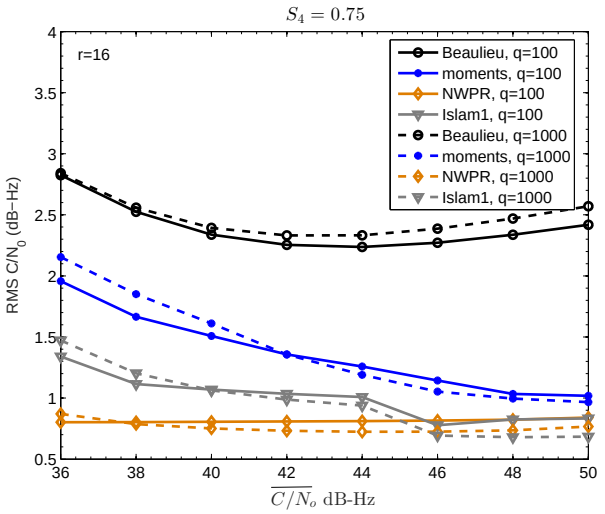

Figure 10: Estimation rms errors of the C/N_0 estimates for different estimators and $\overline{C/N_0}$ values.

of the instantaneous C/N_0 for different values of the scintillation index S_4 and $\overline{C/N_0}$. Without loss of generality, the simulations performed in this paper assumed a Rice distribution for the amplitude fading.

It is shown that, in terms of the performance of the algorithms, the NWPR estimator, a standard solution in scintillation-free scenarios, is a good choice for all the different cases, but the first order Islam's method is a very close solution, including even better bias properties. The moments method has a degraded performance in low scintillation situations and in low $\overline{C/N_0}$ scenarios, as in the paper it needs to compute second and fourth order moments with only 20 samples due to the faster dynamics present in the scintillation process. Finally, the Beaulieu's method presents also a degraded performance when the scintillation level increases, and has more problems in coping with the deep fading present in scintillation environments.

ACKNOWLEDGMENTS

The work of Fernando Nunes and Fernando Sousa was supported by the Portuguese Science and Technology Foundation under Project UID/EEA/50008/2013, and the work of José Marçal was also supported by the Portuguese Science and Technology Foundation under the grant SFRH/BD/105545/2014.

REFERENCES

[1] T. Humphreys, B. Ledvina, M. Psiaki, P. Kintner, "Analysis of ionospheric scintillations using wideband GPS L1 C/A signal data", ION GNSS 2004, Long Beach, CA, pp. 399-407.

[2] T. E. Humphreys, M. L. Psiaki, J. C. Hinks, B. O'Hanlon, P. M. Kintner, "Simulating ionosphere-

induced scintillation for testing GPS receiver phase tracking loops", IEEE J. Sel. Top. Signal Process., vol. 3, no. 4, pp. 707-715, 2009.

[3] A. Dierendonck, "GPS Receivers" (chapter 8), Global Positioning System: Theory and Applications (vol. I), AIAA, Washington DC, 1996.

[4] E. Falletti, M. Pini, L. Lo Presti, "Low complexity carrier-to-noise ratio estimators for GNSS digital receivers", IEEE Trans. Aerospace and Electronic Systems, vol. 47, no. 1, January 2011, pp. 420-437.

[5] B. Anderson, J. Moore, Optimal Filtering, Prentice-Hall, N. Jersey, 1979.

[6] A. Islam, E. Lohan, M. Renfors, "Moment based CNR estimators for BOC/BPSK modulated signal for Galileo/GPS", 5th Workshop on Positioning, Navigation and Communication 2008, WPNC'08, pp. 129-136, 2008.

[7] R. Conker, M. El-Arini, M. Bakry, C. Hegarty, T. Hsiao, Radio Science, "Modeling the effects of ionospheric scintillation on GPS/Satellite-based augmentation system availability", vol. 3, pp. 1-23, 2003.

[8] A. Gelb (edt.), Applied Optimal Estimation, The M.I.T. Press, Cambridge, MA, 1986.

[9] H. Rauch, F. Tung, C. Striebel, "Maximum likelihood estimates of linear dynamic systems", AIAA Journal, vol. 3, no. 8, August 1965, pp. 1445-1450.